Estimation of Cumulative Deformation Capacity of Buckling Restrained Braces

Toru Takeuchi, A.M.ASCE[1]; Mari Ida[2]; Satoshi Yamada[3]; and Kazuaki Suzuki[4]

Abstract: Recently, passive vibration control design has gained popularity. The aim of this design is to absorb most of the seismic energy by using additional dampers while maintaining the elasticity of the main structure. Buckling restrained braces (BRBs) are used as one of the elastoplastic dampers in this design and, therefore, the cumulative deformation capacity of BRBs to the point of fatigue fracture is an important benchmark for their performance. The estimation of this value under a random amplitude is complicated however, as this value is affected by the loading history. In this study, past experiments on BRBs are revisited in order to investigate the relation between the cumulative deformation capacity and the applied loading history. Based on these analyses, a simple method is proposed for predicting the cumulative deformation and energy absorption capacities of BRBs under random amplitudes. In contrast to Miner's method, the proposed method does not require analyses of the individual amplitudes, and the values of interest are directly determined from the response indexes.

DOI: 10.1061/(ASCE)0733-9445(2008)134:5(822)

CE Database subject headings: Elastoplasticity; Random waves; Deformation; Bracing; Energy; Fatigue; Steel structures; Cyclic tests; Buckling.

Introduction

Recently, passive vibration control design has been widely used in areas of higher seismicity, as in Japan. The aim of this design is to absorb most of the seismic energy through additional dampers while maintaining the elasticity of the main structure (Fig. 1). This concept achieves damage control design and can enhance the building property value after a significant seismic event. Buckling restrained braces (BRBs) (Fig. 2), which are described as ductile structural braces in seismic provision for structural steel buildings (AISC 2005), can also be used as one of the elastoplastic dampers. In the United States, the buildings incorporating BRBs as ductile structural braces have been constructed since 2000. Black et al. (2004) have verified the performance of BRBs by experiments under various loading histories and indicated that the cumulative deformation capacity varies with the applied loading history. Aiken et al. (2000) have conducted a low-cycle fatigue test to the point of fracture, and Carden et al. (2006) have estimated the cumulative plastic ductilities until failure under an increasing amplitude loading. On the other hand, in Japan, BRBs are often used as energy dissipation devices provided in moment frames, which dissipate most of the seismic energy input into a building in an effort to maintain the main structure in the elastic range. In such systems, the cumulative deformation capacity of BRBs, prior to the fatigue fracture, is an important benchmark for their performance. Consequently, several experiments have been conducted to the point of fracture both under a constant strain amplitude (Nakamura et al. 2000), and random strain amplitudes simulating seismic response (Hasegawa et al. 1999) in order to investigate the problem. The point of fatigue fracture of these BRBs has been analyzed in relation to the imposed amplitude. However, the amplitude of the actual seismic response is randomly distributed. The estimation of the cumulative deformation capacity under random amplitudes is

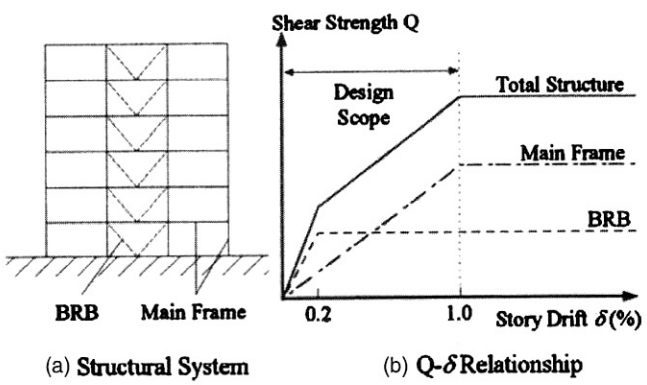

Fig. 1. Concept of damage control design

[1]Associate Professor, Dept. of Architecture and Building Engineering, Tokyo Institute of Technology, M1-29, 2-12-1 O-okayama, Meguro-ku, Tokyo 152-8552, Japan. E-mail: ttoru@arch.titech.ac.jp

[2]Graduate Student, Dept. of Architecture and Building Engineering, Tokyo Institute of Technology, M1-29, 2-12-1 O-okayama, Meguro-ku, Tokyo 152-8552, Japan.

[3]Associate Professor, Structural Engineering Research Center, Tokyo Institute of Technology, 4259 Nagatsuda, Midori-ku, Yokohama-shi, Kanagawa 226-8503, Japan.

[4]Manager, Building Materials and Engineering Service Dept., Nippon Steel Corporation, Ohtemachi 2-6-3, Chiyoda-ku, Tokyo 100-8071, Japan.

Note. Associate Editor: Rakesh K. Goel. Discussion open until October 1, 2008. Separate discussions must be submitted for individual papers. To extend the closing date by one month, a written request must be filed with the ASCE Managing Editor. The manuscript for this paper was submitted for review and possible publication on June 27, 2006; approved on May 8, 2007. This paper is part of the *Journal of Structural Engineering*, Vol. 134, No. 5, May 1, 2008. ©ASCE, ISSN 0733-9445/2008/5-822–831/$25.00.

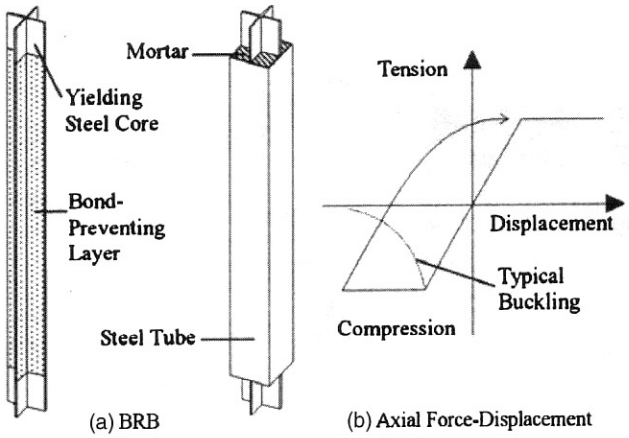

Fig. 2. Schematic diagram of BRB

complicated, as this value is also affected by the loading history. Miner's method can be used to estimate this value; however, it requires analyses of individual vibration amplitudes and is not necessarily precise, particularly in large strain ranges, as reported by Nakagomi and Lee (1995). In the present study, past experiments on BRBs conducted by the authors are analyzed by decomposing hysteretic loops into "skeleton part" and "Bauschinger part," as proposed by Kato et al. (1973), and the relation between the cumulative deformation capacity and the loading history is discussed. Further, based on these analyses, a simple method is proposed to predict the cumulative deformation capacity and energy dissipation capacity of BRBs subjected to random amplitudes.

Fatigue Curve and Miner's Method

Fig. 3 shows the past experiments conducted on BRBs considered here and their loading histories. The experiments include a constant amplitude fatigue test (Nakamura et al. 2000), a shaking table test of a BRB component (Hasegawa et al. 1999), a shaking table test of a BRB frame and a component test under random amplitudes record (Yamaguchi et al. 2002, 2004), and a test of a truss frame under a gradually increasing amplitude (Takeuchi et al. 2005). All tests are conducted to the point of fracture, which is defined as the point that the strength degradation over 25% to the maximum strength has been observed in the hysteretic loop, in order to determine the cumulative deformation capacity of the BRB core. The details and results of the tests are summarized in Table 1 and Fig. 4. The minimum specified values of mechanical properties for Japanese steel grades are shown in Table 2. In Fig. 4, the shaking table tests and the BRB component tests subjected to random amplitudes record are categorized as shaking table tests. The cumulative strain values to the point of fracture are widely distributed, depending on loading histories and cannot be estimated as constant values. The results of a constant amplitude fatigue test clearly show a relationship between the cumulative strain capacity and the strain amplitude. This test is performed on three types of steel materials under various strain zones (from 0.16 to 4.5%). The fatigue curve can be obtained from the results of this test. Manson (1966) and Coffin (1962) have indicated that the number of failure cycles N_f and each strain amplitude on steel materials can be expressed as follows:

$$\Delta\varepsilon_e = C_1 \times N_f^{m1} \tag{1}$$

$$\Delta\varepsilon_p = C_2 \times N_f^{m2} \tag{2}$$

$$\Delta\varepsilon_t = C_1 \times N_f^{m1} + C_2 \times N_f^{m2} \tag{3}$$

where $\Delta\varepsilon_e$=elastic strain amplitude; $\Delta\varepsilon_p$=plastic strain amplitude; $\Delta\varepsilon_t$=total strain amplitude; and C_i and m_i=constants that depend on the material. Each strain amplitude of a hysteretic loop is defined in Fig. 5. Previous studies (Maeda et al. 1998; Nakagomi et al. 2000) have shown that these equations can be applied to the BRB core. Plastic strain is generally distributed over the entire length of the core plates when sufficient restraint against buckling is provided and the core maintains positive incremental stiffness after its yield. The Manson-Coffin equations can be applied under this assumption. Fig. 6 shows the fatigue curve obtained from the constant amplitude fatigue test. It shows that the fatigue properties of BRBs are not significantly affected by steel material and Eq. (3) for BRBs can be expressed approximately as

$$\Delta\varepsilon_t = 0.5 \times N_f^{-0.14} (\Delta\varepsilon_t < 0.1) \tag{4}$$

$$\Delta\varepsilon_t = 20.48 \times N_f^{-0.49} (0.1 \leqq \Delta\varepsilon_t < 2.2) \tag{5}$$

$$\Delta\varepsilon_t = 54.0 \times N_f^{-0.71} (2.2 \leqq \Delta\varepsilon_t) \tag{6}$$

These equations cannot be used directly for the response analysis when subjected to random amplitudes. As one method to apply them to random amplitudes, Miner (1945) has defined a failure condition based on the following equation. Under this condition, when the cumulative "damage" of individual amplitudes reaches 1.0, the element sustains fatigue fracture

$$D = \sum_{i=1}^{n} \frac{n_i}{N_{\mathrm{fi}}} = 1.0 \tag{7}$$

where n_i=number of cycles for the strain amplitude $\Delta\varepsilon_i$; N_{fi}=number of failure cycles for $\Delta\varepsilon_i$; and D=damage index. The original concept has been applied to the stress-N_f curve; however, it is also commonly applied to the strain-N_f curve, as shown in Fig. 6. In this study, first, the fracture conditions in each test are predicted by this method. The frequencies of random amplitudes are calculated by the rain flow method, which is known as one of the stress frequency count methods. The principle of this method is shown in Fig. 7, where the vertical and the horizontal axis means the time and the strain, respectively. In this method, the amplitudes are counted by simplifying the random record in imitating a stream line that flows from a source of each extremum and those that skipped from the record are counted as shown in Fig. 7(b). An example of the frequency distribution of amplitudes from a shaking table test is shown in Fig. 8. From these amplitudes, the values of D to the point of fracture are calculated using Eq. (7). Fig. 9 shows the result of each test. The D values at the point of fracture are distributed from 0.29 to 1.68, and they are not necessarily precise. In particular, the D value estimated by the test with a gradually increasing amplitude, which has the most large average strain amplitude around 4% compared with the other tests almost under 2%, is three times less than the predicted value. Another report (AIJ 2004) has indicated that the accuracy of Miner's method for an element under large plastic strains could vary from 0.05 to 1.2; this is consistent with the results of the present study. Moreover, Miner's method requires analyses

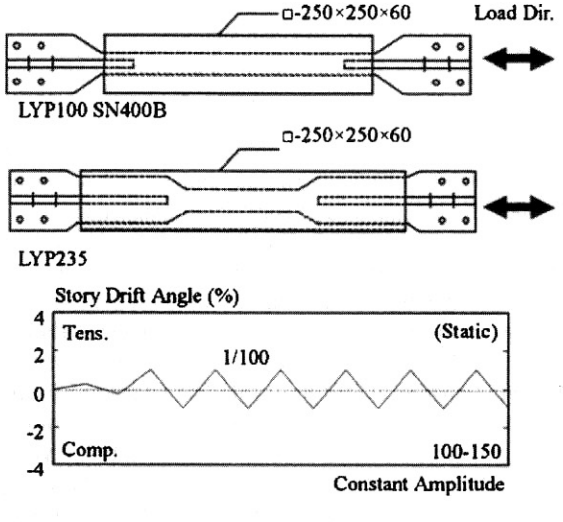

Constant Amplitude Fatigue Test
(Nakamura et al. 2000)

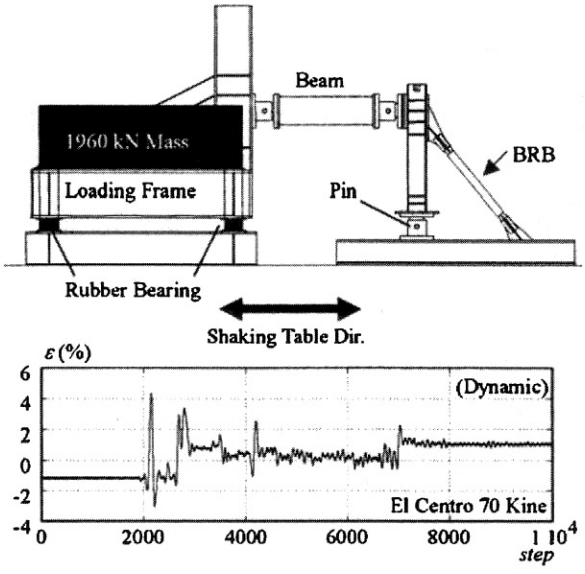

Shaking Table Test of Component
(Hasegawa et al. 1999)

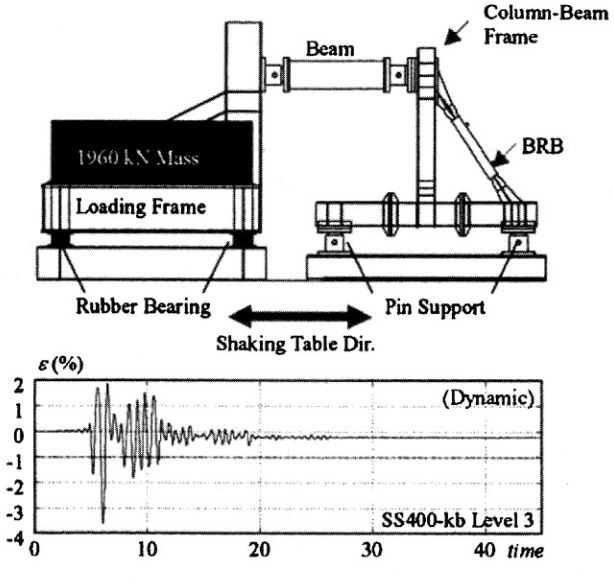

Shaking Table Test BRB Frame
(Yamaguchi et al. 2002)

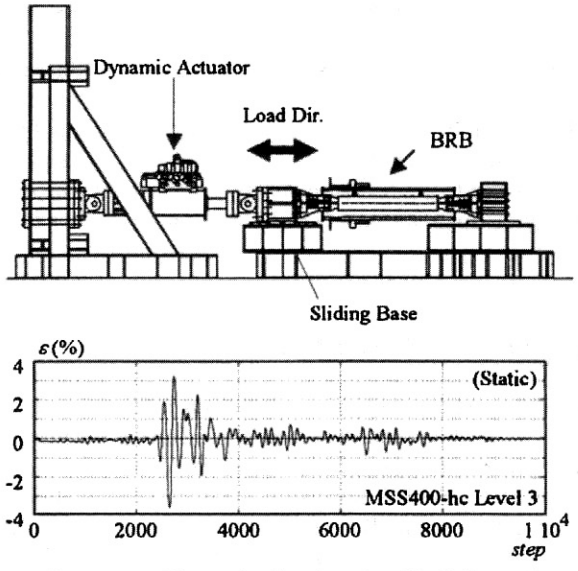

Component Test under Random Amplitude Record
(Yamaguchi et al. 2004)

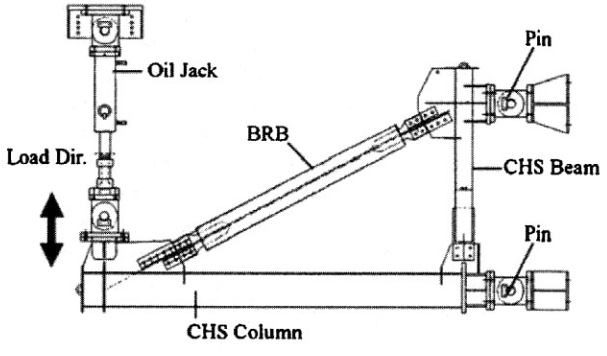

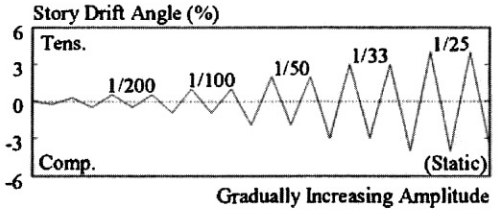

Test with Gradually Increasing Amplitude
(Takeuchi et al. 2005)

Fig. 3. Past experiments on BRBs

Table 1. Specimen Summary of Past Tests on BRBs

Test	Specimen	Steel	Core plate	Thickness (mm)	Width (mm)	Length (mm)	Input ε (%)	ε_{max} (%) Tens.	ε_{max} (%) Comp.	$\overline{\Delta\varepsilon_{ph}}$ (%)
Constant amplitude	100−150	LY100	−	25	100	960	1.5	0.76	−0.79	0.68
fatigue test	100−016	LY100	−	25	100	960	0.16	0.10	−0.08	0.02
	100−040	LY100	−	25	100	960	0.4	0.21	−0.21	0.13
	100+150	LY100	+	25	100	1,180	1.5	0.73	−0.79	0.69
	400−200	SN400B	−	25	100	960	2	1.01	−0.99	0.82
	400−150	SN400B	−	25	100	960	1.5	0.78	−0.79	0.56
	235+150	LY225	+	16	100	470	4.3	2.11	−2.26	1.86
	235+150	LY225	−	28	100	470	4.5	2.21	−2.38	2.01
Shaking table test of component	El Centro	SS400	−	22	130	1,291	E.C.[a]	6.93	−3.10	0.33
Shaking table test	SS400-	SS400	−	16	60	1,200	kb,hc[b]	6.55	−5.99	0.51
BRB frame	LYP100	LY100	−	16	75	1,200	kb,hc[b]	5.16	−5.47	0.30
	LYP235	LY225	−	16	75	600	kb,hc[b]	6.98	−5.96	0.59
Component test under	M SS400-	SS400	−	16	60	1,200	kb,hc[b]	5.14	−5.46	0.49
random amplitude	M LYP100	LY100	−	16	75	1,200	kb,hc[b]	2.51	−5.30	0.28
record	M LYP235	LY225	−	16	75	600	kb,hc[b]	7.04	−5.94	0.71
Test with gradually	TB-1	LY225	−	16	92	1,370	Normal	4.40	−3.64	1.94
increasing amplitude	TAS-1	LY225	−	16	92	1,370	Normal	3.94	−3.93	2.04
	TAS-1′	LY225	−	16	92	1,370	Near field	3.60	−5.16	1.89
	TAS-2	LY225	−	16	58	1,610	Normal	3.15	−3.31	1.69
	TAS-2′	LY225	−	16	58	1,610	Near field	4.01	−4.12	1.61

[a]El Centro NS.

[b]JM A Kobe NS, Hachinohe NS.

of individual amplitudes, a difficult task when considering standard response histories.

Estimation of Cumulative Strain Capacity with Skeleton Ratio

There is an idea that the hysteretic loop of a steel element can be decomposed into the skeleton part and the Bauschinger part (Fig. 10). The skeleton part is defined as a part in which the specific level of stress occurs for the first time, and the Bauschinger part is others except the elastic unloading part. Kato and Akiyama (Kato et al. 1973; Akiyama et al. 1995) have shown that the deformation capacity is strongly related to the addition of the skeleton part that matches in the stress-strain curve of the tensile test. The cumulative strain of each part is shown in Fig. 4. The ratio of the skeleton part to the cumulative plastic strain reaches 20% in the test with a gradually increasing amplitude, while in all other tests, it is less than 10%. A higher ratio of the skeleton part apparently leads to a lower cumulative strain capacity.

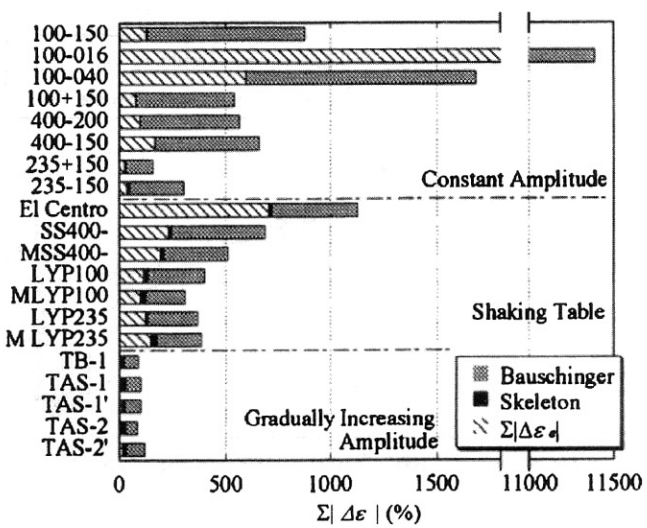

Fig. 4. Cumulative strain to point of fracture

Based on the above characteristics, a method is developed for estimating the cumulative strain capacity. By assuming that the hysteretic loop is expressed as a simple bilinear model (Fig. 5) and the loop is repeated N_f times prior to the fatigue fracture, each part can be expressed as follows:

$$\chi = 4\Delta\varepsilon_{ph}N_f \tag{8}$$

$$\chi_S = 3\Delta\varepsilon_{ph} \tag{9}$$

$$\chi_B = \chi - \chi_S = 4\Delta\varepsilon_{ph}(N_f - 0.75) \tag{10}$$

where χ=cumulative plastic strain; χ_s=skeleton part; χ_B=Bauschinger part; and $\Delta\varepsilon_{ph}$=half of the plastic strain amplitude (Fig. 5).

By substituting N_f obtained from Eq. (8) into Eq. (2), the cumulative plastic strain under a constant amplitude is given by

$$\Delta\varepsilon_{ph} = \frac{1}{2}\Delta\varepsilon_p = \frac{1}{2}C_2 \times N_f^{m_2} = C \times N_f^{m_2} \tag{11}$$

$$\ln \Delta\varepsilon_{ph} = \ln C + m_2 \ln \frac{\chi}{4\Delta\varepsilon_{ph}} \tag{12}$$

Table 2. Minimum Specified Values of Mechanical Properties for Japanese and Comparable U.S. Steel Grades

Steel grade	Steel type	Minimum specified values of mechanical properties			
		f_y (MPa)	0.2% f_y (MPa)	f_u (MPa)	ε_u (%)
Japanese steel grade: SS400 (JIS)	Carbon steels for general structure	245[a]	—	400–510	17[a]
Comparable U.S. steel grade: A36 (ASTM)	Carbon steels for general structure	250		400–550	20
Japanese steel grade: SN400B (JIS)	Carbon steels for building structure	235–355[b]	—	400–510	22[b]
Comparable U.S. steel grade: A1043/A (ASTM)	Carbon steels for building structure	250–360		400	23
Japanese steel grade: LY100[c]	Low-yield-strength steel	—	80–120	200–300	50
Japanese steel grade: LY225[c]	Low-yield-strength steel	215–245	—	300–400	40
Comparable U.S. steel grade:	—	—	—	—	—

[a]Range of thickness: 16 (mm) and under.

[b]Over 16 (mm) and under 40 (mm).

[c]Ministerial approved standard.

$$\chi = 4\left\{\frac{C}{\Delta\varepsilon_{\text{ph}}^{(1+m_2)}}\right\}^{-\frac{1}{m_2}} \tag{13}$$

By assuming that the extent of damage in the skeleton part is a times that in the Bauschinger part, Eq. (13) can be rewritten as

$$\chi = a\chi_S + \chi_B = 4\left\{\frac{C}{\Delta\varepsilon_{\text{ph}}^{(1+m_2)}}\right\}^{-\frac{1}{m_2}} \tag{14}$$

When fatigue fracture occurs only due to the skeleton part without the Bauschinger part, the cumulative strain, denoted by χ_{SO}, is given by

$$a\chi_{SO} = 4\left\{\frac{C}{(\Delta\varepsilon_{\text{ph}})^{(1+m_2)}}\right\}^{-\frac{1}{m_2}} \tag{15}$$

By substituting a obtained from Eq. (15) into Eq. (14), the fracture condition can be expressed as

$$\frac{\chi_S}{\chi_{SO}} + \frac{\chi_B}{4}\left\{\frac{\Delta\varepsilon_{\text{ph}}^{(1+m_2)}}{C}\right\}^{-\frac{1}{m_2}} = 1.0 \tag{16}$$

With skeleton ratio α_s defined as the ratio of χ_s to χ

$$\alpha_s = \frac{\chi_S}{\chi} \tag{17}$$

and χ_B given by

$$\chi_B = (1-\alpha_S)\chi \tag{18}$$

Eq. (16) can be rewritten

$$\chi = \frac{1}{\dfrac{\alpha_S}{\chi_{SO}} + \dfrac{(1-\alpha_S)}{4}\left\{\dfrac{\overline{\Delta\varepsilon_{\text{ph}}}^{(1+m_2)}}{C}\right\}^{-\frac{1}{m_2}}} \tag{19}$$

where $\overline{\Delta\varepsilon_{\text{ph}}}$=half of the average plastic strain amplitude. In Eq. (19), $\Delta\varepsilon_{\text{ph}}$ is replaced with $\overline{\Delta\varepsilon_{\text{ph}}}$ for applying it to the random amplitude response.

By using Eq. (19), the cumulative strain capacity can be directly calculated. The constant C and m_2 are obtained from a constant amplitude fatigue test and these values for BRBs are determined as 27 and −0.71, respectively, from Eq. (6). Another constant χ_{SO}, the cumulative plastic strain to the point of fatigue fracture especially brought only by the skeleton part, is regarded as a simple tensile test. Consequently, the constant χ_{SO} can be defined as a minimum fracture elongation value in the past coupon tests and it is estimated as 35 (%) in the present study. These constants are substituted into Eq. (19) and the following equation is obtained:

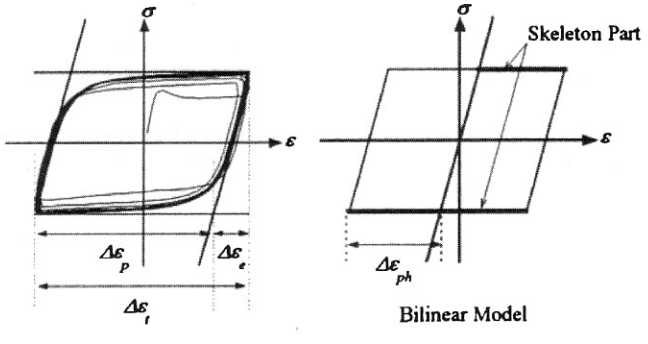

Fig. 5. Hysteretic loop and model

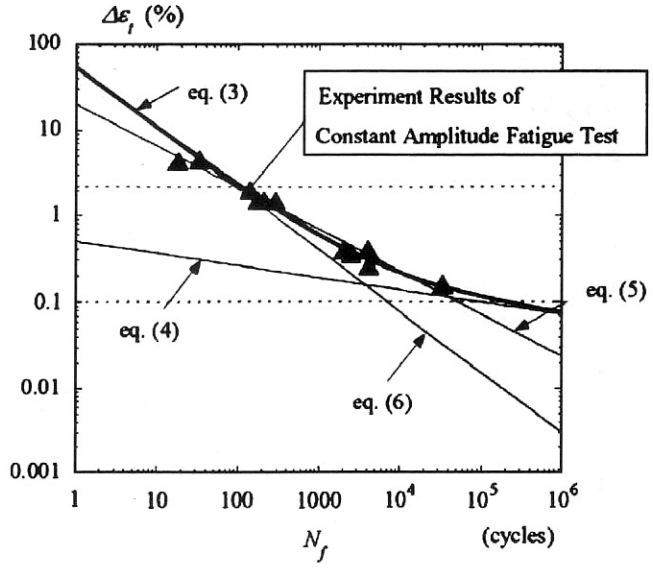

Fig. 6. Relationship between $\Delta\varepsilon_t$ and N_f

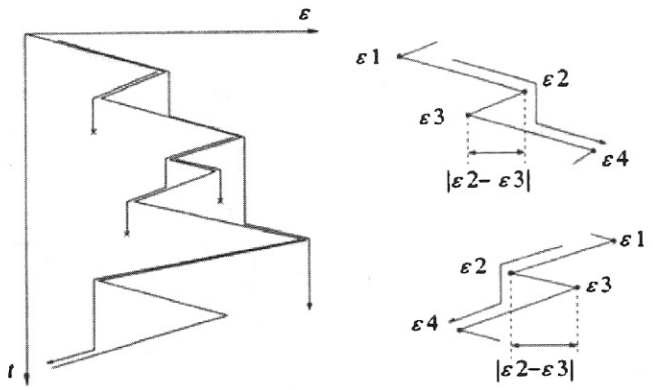

(a) Principle Model (b) Count Method for Skipped Amplitude

Fig. 7. Principle of rain flow method

$$\chi(\%) = \frac{1}{\frac{\alpha_S}{35} + (1-\alpha_S)\left\{\frac{\overline{\Delta\varepsilon_{ph}}^{0.41}}{417.14}\right\}} \tag{20}$$

The value of $\overline{\Delta\varepsilon_{ph}}$ is calculated by the rain flow method. In Fig. 11, the curves of the cumulative strain capacity obtained from Eq. (20) are compared with the experimental results; (a) shows the results of a constant amplitude fatigue test; (b) those of a shaking table test; and (c) those of the test with a gradually increasing amplitude. In the figure, the proposed method is represented by the smooth lines with the marks indicating the results obtained experimentally. In (d) the results of the experiments and proposed method are compared for all three types of loading. Generally, the results calculated using Eq. (20) can effectively predict the experimental results with the corresponding value of $\overline{\Delta\varepsilon_{ph}}$. The variance value for predicted results is calculated as 0.067, based on the experimental results, while that for Miner's method is 0.196. The accuracy of the proposed method is improved in comparison with Miner's method, especially for a range of large strain amplitudes. In Fig. 12, the process of strain accumulation is shown in each experiment. In the shaking table tests, the initial value of α_s is in the range of 0.05–0.35; then, it reduces slightly to around 0.05–0.15 and reaches the fracture lines defined by Eq. (20). On the other hand, in the test with a gradually increasing amplitude, α_s is initially very high around 0.8; subsequently, it reduces to 0.2 and reaches the fracture line. Since the fracture lines shift downward at high values of α_s, a high initial

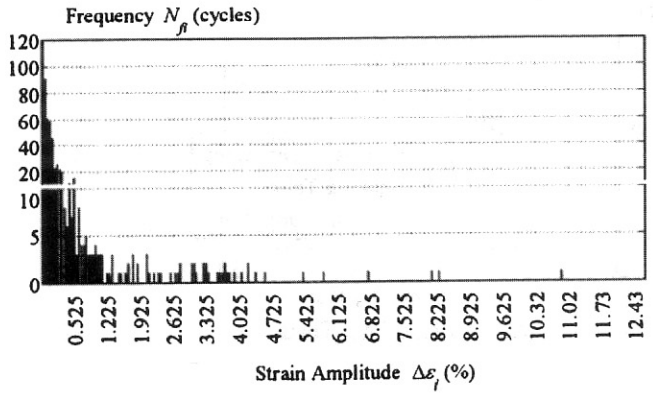

Fig. 8. Amplitude and frequency of shaking table test

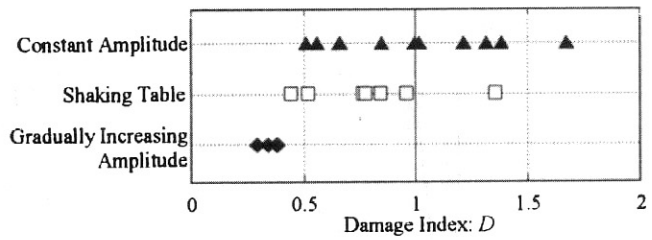

Fig. 9. Accuracy of Miner's method

value of α_s leads to a lower cumulative strain-capacity. For prediction with the proposed method, only the key values of α_s and $\Delta\varepsilon_{ph}$ are required. These values are related to the seismic response amplitude and the stiffness ratio of BRBs to the moment frames. They could be directly estimated from the maximum response of the structure as indicated by Akiyama (1999). Therefore, when these values are obtained, analyses of the individual amplitude of response vibrations, as in the case of Miner's method, are not required for estimating the cumulative strain capacity under random amplitudes.

Estimation of Energy Absorption Capacity

As advocated by Akiyama (1985), the seismic design method, which considers the seismic energy input and energy absorption capacity of the structure, has also gained popularity. It is important to accurately predict the capacity of BRBs to act as energy dissipators. To this end, Eq. (19) can also be used to estimate the energy absorption capacity. The absorbed energy value is calculated by the sum of closed areas of the hysteretic loop, and it is affected by the hardening stiffness after yielding (Fig. 13). Fig. 14 shows the absorbed energy of BRBs to the point of fracture in each experiment. It is evident that the energy absorption capacity of elastoplastic dampers is not constant and is significantly affected by the strain amplitude and loading history, as in the case of the deformation capacity. For predicting the energy absorption capacity, the hardening stiffness ratio β is defined as the ratio of the additional areas due to the hardening stiffness to the areas without hardening; then, β is set to the right side of Eq. (19). The value of β is generally in the range of 1.2–1.5 with an average of 1.37. The absorbed energy of BRBs to the point of fracture is calculated as follows:

$$\chi_w(\%) = \frac{\beta}{\frac{\alpha_S}{35} + (1-\alpha_S)\left\{\frac{\overline{\Delta\varepsilon_{ph}}^{0.41}}{417.14}\right\}} \tag{21}$$

where χ_w=normalized cumulative absorbed energy. This value is obtained by dividing the cumulative absorbed energy by the yield strength.

In Fig. 15, the values of χ_w determined by Eq. (21) are plotted along with those calculated from the hysteretic loops in each experiment. As in the case of the cumulative deformation, χ_w can be estimated effectively by the proposed method. Results obtained using LY100 (indicated by *) are on the conservative side. This is due to a remarkable increase in the yield strength of LY100 steel, which is not estimated by Eq. (21). The mechanical property of LY100 is shown in Table 2. Even in this case, the accuracy of the proposed method has the variance value of 0.166, which is still considered to be acceptable.

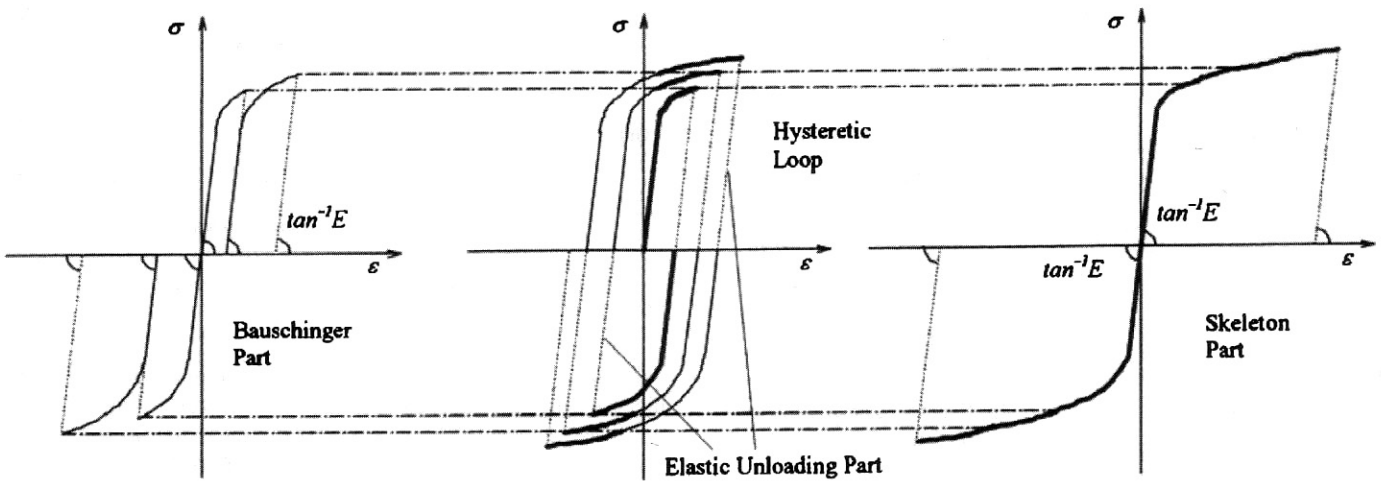

Fig. 10. Decomposition of hysteretic loop

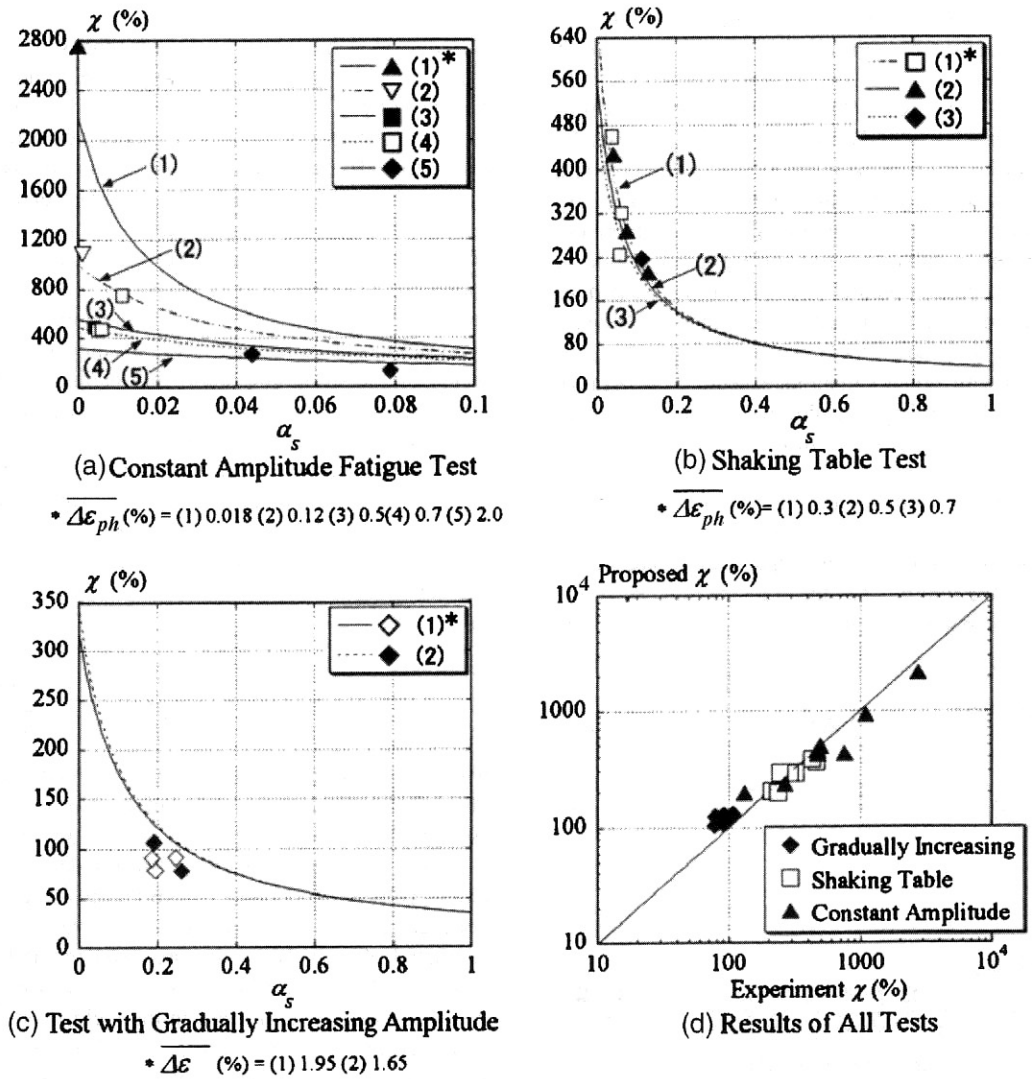

Fig. 11. Comparison between experiment and proposed method (cumulative strain)

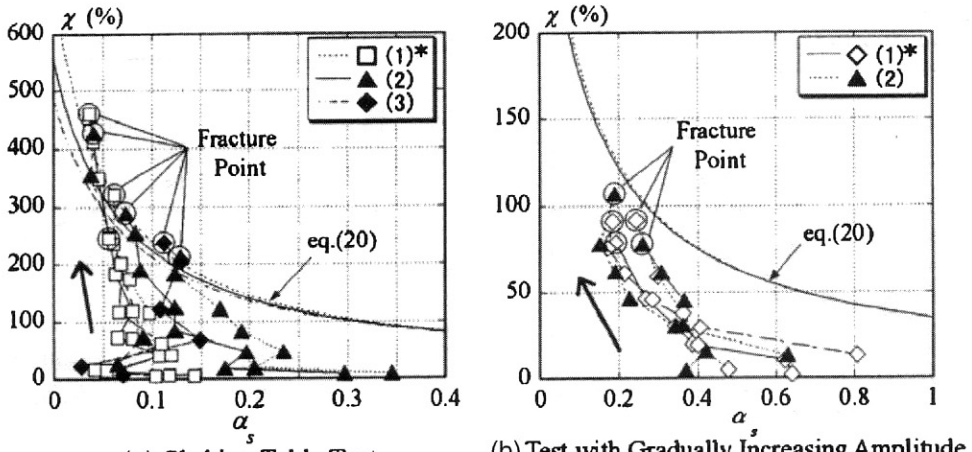

Fig. 12. Shift of skeleton ratio to point of fracture

Discussions on the Proposed Equations

Eq. (19) is derived by assuming that the hysteretic loop of BRB is expressed as a bilinear model and the cumulative plastic strain is given by Eq. (8). In order to redetermine the relationship between $\overline{\Delta\varepsilon_{ph}}$ and N_f, Eq. (8) is substituted into Eq. (19) and the following equations are obtained; $\Delta\varepsilon_{ph}$ in Eq. (8) is replaced with $\overline{\Delta\varepsilon_{ph}}$:

$$\overline{\Delta\varepsilon_{ph}} = \frac{\chi}{4N_f} = \frac{1}{\left\{\frac{4\alpha_S}{\chi_{SO}} + (1-\alpha_S)\left(\frac{\overline{\Delta\varepsilon_{ph}}^{(1+m_2)}}{C}\right)^{-\frac{1}{m_2}}\right\}N_f} \tag{22}$$

$$N_f = \frac{1}{\frac{4\overline{\Delta\varepsilon_{ph}}\alpha_S}{\chi_{SO}} + (1-\alpha_S)\left(\frac{\overline{\Delta\varepsilon_{ph}}}{C}\right)^{-\frac{1}{m_2}}} \tag{23}$$

From Eqs. (8) and (9), α_s can be expressed as

$$\alpha_S = \frac{\chi_S}{\chi} = \frac{3}{4N_f} \tag{24}$$

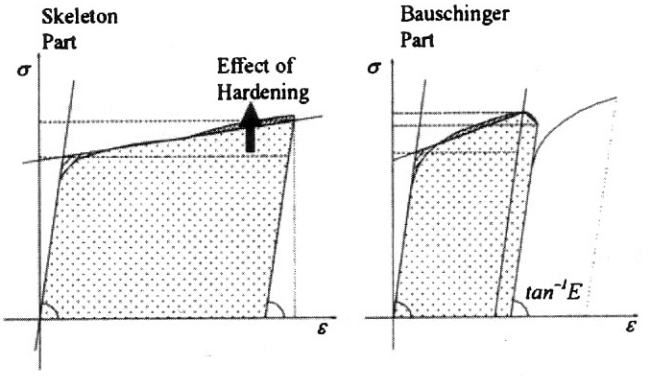

Fig. 13. Calculation of absorbed energy

By substituting Eq. (23) into Eq. (24), N_f is obtained as follows:

$$N_f = \left(1 - \frac{3\overline{\Delta\varepsilon_p}}{2\chi_{SO}}\right)\left(\frac{\overline{\Delta\varepsilon_p}}{C_2}\right)^{\frac{1}{m_2}} + 0.75 \tag{25}$$

where $\overline{\Delta\varepsilon_p}$=average plastic strain amplitude ($\overline{\Delta\varepsilon_p}=2\overline{\Delta\varepsilon_{ph}}$).

Hence, the fatigue curve of the large strain range is expressed by Eq. (25). When α_s is estimated as 1, which implies that χ_{SO} is equal to $3\overline{\Delta\varepsilon_p}/2$, N_f is calculated as 0.75. On the contrary, when N_f approaches infinity, which implies that $\overline{\Delta\varepsilon_p}$ approaches 0, Eq. (25) is simplified as

$$N_f = \left(\frac{\overline{\Delta\varepsilon_p}}{C_2}\right)^{\frac{1}{m_2}} + 0.75 \tag{26}$$

Under this assumption, the second term is considered to be negligible. Therefore, Eq. (26) can be expressed as

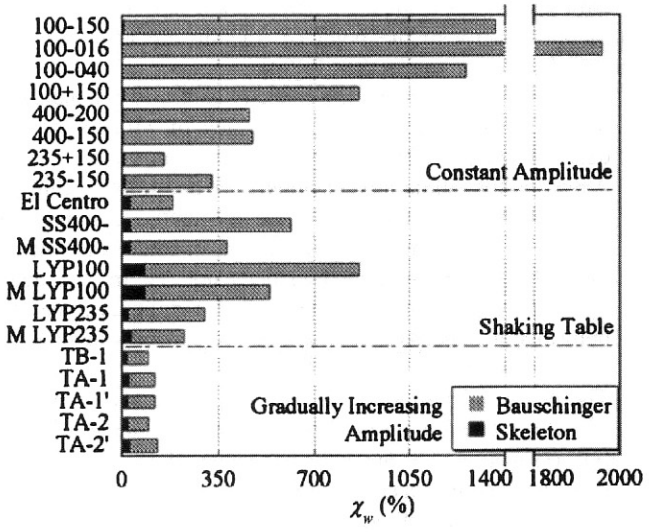

Fig. 14. Cumulative absorbed energy

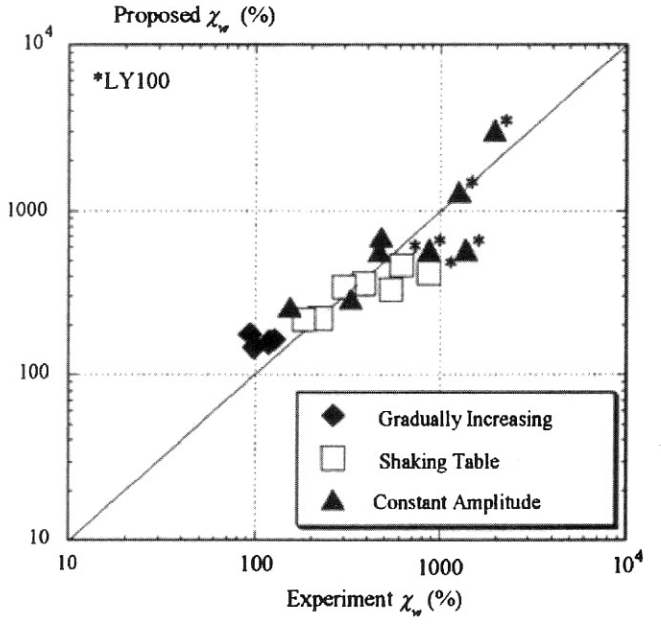

Fig. 15. Comparison between experiment and proposed method (cumulative absorbed energy)

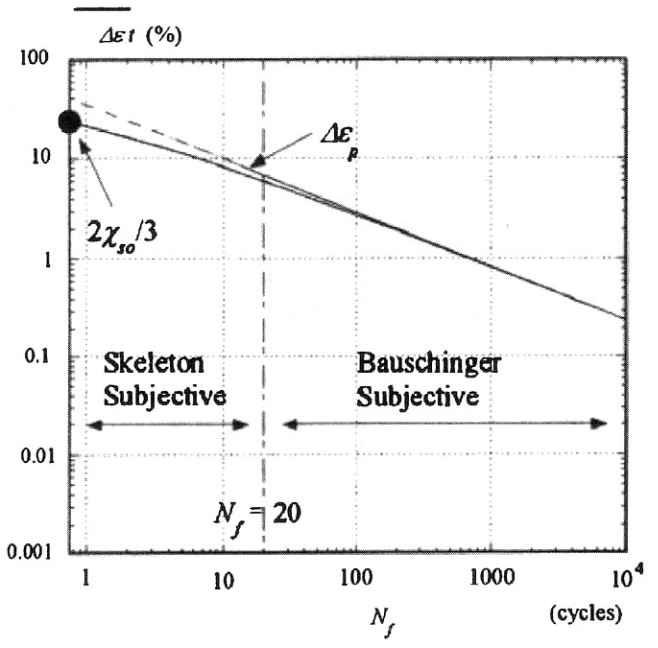

Fig. 16. Fatigue curve model under high strain range

$$N_f = \left(\frac{\overline{\Delta\varepsilon_p}}{C_2}\right)^{\frac{1}{m_2}} \tag{27}$$

This equation is the same as Eq. (2), in which $\Delta\varepsilon_p$ is replaced with $\overline{\Delta\varepsilon_p}$. These properties are included in Eq. (19). When N_f approaches infinity, Eq. (27) approximates the Manson-Coffin equation, and when N_f is equal to 0.75, it converges on a certain strain amplitude produced by the fracture of only the skeleton parts. The model of the fatigue curve is shown in Fig. 16. In the range of N_f under 20, the plot diverges from the Manson-Coffin equation. Uneven distributions of large plastic strains are considered to be one of the reasons for this divergence.

Conclusions

Past experiments conducted on buckling restrained braces (BRBs) are studied, and their cumulative deformation capacity and energy absorption capacity to the point of fracture are analyzed. The main results are summarized as follows:

1. The cumulative deformation capacity is clearly dependent on the deformation history. The accuracy of Miner's method decreases considerably at larger plastic strains.
2. A method for estimating the cumulative deformation capacity is proposed by decomposing the hysteretic loop into the skeleton part and the Bauschinger part. In contrast to Miner's method, the proposed method does not require the determination of damage with individual amplitudes, and the deformation capacity can be directly calculated when the key values of α_s and $\overline{\Delta\varepsilon_{ph}}$ are obtained.
3. The energy absorption capacity of BRBs can also be estimated by determining the hardening effect. The accuracy of this estimation has the variance value of 0.166, which is considered to be acceptable for practical design.
4. In the proposed method, the properties of a large strain amplitude are expressed in terms of the divergence from fatigue curves in the range of N_f under 20.

The key values required for the proposed method are considered to be related to the seismic response amplitude and the stiffness ratio of BRBs to the moment frames. Simple methods for estimating these values using the maximum responses will be described in future studies.

Notation

The following symbols are used in this paper:

a = damage ratio of the skeleton part;
C_i = constant of fatigue curve;
D = damage index of Miner's method;
m_i = constant of fatigue curve;
N_f = number of failure cycles;
α_S = skeleton ratio;
β = hardening stiffness ratio;
$\Delta\varepsilon_e$ = elastic strain amplitude;
$\Delta\varepsilon_t$ = total strain amplitude;
$\Delta\varepsilon_p$ = plastic strain amplitude;
$\overline{\Delta\varepsilon_p}$ = average plastic strain amplitude;
$\Delta\varepsilon_{ph}$ = half of the plastic strain amplitude;
$\overline{\Delta\varepsilon_{ph}}$ = half of the average plastic strain amplitude;
χ = cumulative plastic strain;
χ_B = cumulative plastic strain of the Bauschinger part;
χ_s = cumulative plastic strain of the skeleton part;
χ_{so} = cumulative plastic strain to the point of fatigue fracture brought only by the skeleton part; and
χ_w = normalized cumulative absorbed energy.

References

AIJ. (2004). "Loading effect and fatigue failure by wind and earthquake." *Proc., AIJ Committee Symp. on Effect of Repeated Load*, AIJ, Tokyo, 33–39 (in Japanese).

Aiken, I. D., Clark, P. W., Tajirian, F. F., Kasai, K., Kimura, I., and Ko, E. (2000). "Unbonded braces in the United States—Design studies,

large-scale testing, and the first building application." *Proc., Japan Passive Control Symp.*, Tokyo Institute of Technology, Japan, 203–217.

AISC. (2005). "Seismic provisions for structural steel buildings including supplement No. 1." *AISC Publication C16 Buckling-Restrained Braced Frames*, American Institute of Steel Construction, Inc., Chicago, 204–207.

Akiyama, H. (1985). *Earthquake resistant limit-state design for buildings*, University of Tokyo Press, Tokyo.

Akiyama, H. (1999). *Earthquake-resistant design method for buildings based on energy balance*, Gihodo Press, Tokyo (in Japanese).

Akiyama, H., Takahashi, M., and Shi, Z. (1995). "Ultimate energy absorption capacity of round-shape steel rods subjected to bending." *J. Struct. Constr. Eng.*, 475, 145–154 (in Japanese).

Black, C. J., Makris, N., and Aiken, I. D. (2004). "Component testing, seisimic evaluation, and characterization of buckling-restrained braces." *J. Struct. Eng.*, 130(6), 880–894.

Carden, L. P., Itani, A. M., and Buckle, I. G. (2006). "Seismic performance of steel girder bridges with ductile cross frames using buckling-restrained braces." *J. Struct. Eng.*, 132(3), 338–345.

Coffin, L. F., Jr. (1962). "Experimental support for generalized equation predicting low cycle fatigue." *J. Basic Eng.*, 84, 533–537.

Hasegawa, H., Takeuchi, T., Iwata, M., Yamada, S., and Akiyama, H. (1999). "Dynamic performances of unbonded braces." *AIJ Technical Rep. No. 9*, 103–106 (in Japanese).

Kato, B., Akiyama, H., and Yamanouchi, Y. (1973). "Experimental low of stress-strain curve of steel material." *Proc., AIJ Annual Meeting*, AIJ, Tokyo, 937–938 (in Japanese).

Maeda, Y., Nakata, Y., Iwata, M., and Wada, A., (1998). "Fatigue properties of axial-yield type hysteresis dampers." *J. Struct. Constr. Eng.*, 503, 109–115 (in Japanese).

Manson, S. S. (1966). *Thermal stress and low cycle fatigue*, McGraw-Hill, New York.

Miner, M. A. (1945). "Cumulative damage in fatigue." *J. Appl. Mech.*, 12, 159–164.

Nakagomi, T., Iwamoto, T., Kamura, H., Shimokawa, H., and Harayama, K. (2000). "Experimental study on fatigue characteristic of flat-bar brace with low yield stress steel stiffened by square steel tube." *J. Struct. Constr. Eng.*, 530, 155–161 (in Japanese).

Nakagomi, T., and Lee, K. (1995). "Experimental study on fatigue characteristic of SM490 by repeated load." *J. Struct. Constr. Eng.*, 469, 127–136 (in Japanese).

Nakamura, H., et al. (2000). "Fatigue properties of practical-scale unbonded braces." *Nippon Steel Technical Rep. No. 82*, 51–57.

Takeuchi, T., Uchiyama, T., Suzuki, K., Ookouchi, Y., Ogawa, T., and Kato, S. (2005). "Seismic retrofit of truss tower structures using buckling restrained braces." *J. Struct. Constr. Eng.*, 589, 129–136 (in Japanese).

Yamaguchi, M., et al. (2002). "Shaking table test of damage controlled frame with buckling restrained braces." *J. Struct. Constr. Eng.*, 558, 189–196 (in Japanese).

Yamaguchi, M., Yamada, S., Takeuchi, T., and Wada, A. (2004). "Seismic performance of buckling resistant brace within a steel frame in the case of ultimate earthquake." *J. Constructional Steel*, 12, 207–210 (in Japanese).